

RESEARCH PAPER

The Role of Tannic Acid as Reducing and Capping Agent in Phytosynthesis of Zinc Oxide Nanoparticles for Anti-Cancer Activity

Taha A. Ahmed ^{1*}, Raghad Dhyea Abdul Jalill ¹, Azhar M. Haleem ²

¹ Department of Biology, College of Science, AL-Mustainsiriyah University, Baghdad, Iraq

² Environmental Research Center, University of Technology, Baghdad, Iraq

ARTICLE INFO

Article History:

Received 09 October 2024

Accepted 21 December 2024

Published 01 January 2025

Keywords:

Green-synthesis

HSSC

Lymphocyte

Mitotic index

ZnONPs

ABSTRACT

In the present study, ZnONPs were synthesized using Tannic acid. During phytosynthesis of ZnONPs, the color of the solution changed from colorless to red color. Our analysis of UV test, found that maximum absorption is at 268 nm. The obtained four energy band gaps of 0.85, 1.25, 2.45 and 3 eV Indicate the presence of two quantitative wells. The functional groups present on the surface of TA and ZnONPs were investigated by FTIR analysis, the results found that there were more than five bands in synthesized ZnONPs were shifted towards higher or lower than that found in the standard pure of Tannic acid which is good evidence for the success of the reaction between tannic acid and ZnONPs. The result of XRD analysis found hexagonal structure nanoparticles which have 27.2 nm calculating by Sherrer equation. The size which measured by AFM was 38.18 nm, root mean square (Sq) was 18.28 nm, maximum height 162.4 nm, Arithmetic mean height 3.84 nm. SEM image of ZnONPs found rod shape particles. The prepared zinc oxide nanoparticles were assessed for their toxicological effect on the human skin squamous carcinoma cell line (HSSC) in pass 27 and human oral squamous carcinoma cell line (HOSC) in pass 22. For HSSC cell line, the IC50 was 200, 200, and 150 µg/mL for the periods of incubation of 24, 48, and 72 hours, respectively. For HOSC cell line, the IC50 was 225, 182, and 167 µg/mL for the periods of incubation of 24, 48, and 72 hours, respectively. It is evident from the results that the higher concentration of ZnONPs found to inhibit mitotic index, blastogenic index and caused chromosomal aberrations in blood lymphocytes.

How to cite this article

Ahmed T., Jalill R., Haleem A. The Role of Tannic Acid as Reducing and Capping Agent in Phytosynthesis of Zinc Oxide Nanoparticles for Anti-Cancer Activity. J Nanostruct, 2025; 15(1):358-369. DOI: 10.22052/JNS.2025.01.034

INTRODUCTION

Zinc oxide nanoparticles (ZnONPs) are small particles with diameters typically less than 100 nanometers, they are white powder compound which insoluble in water and are versatile semiconductor materials with a wide bandgap

* Corresponding Author Email: taha.a.ahmed@uomustansiriyah.edu.iq

(around 3.37 eV at room temperature) and high surface area-to-volume ratio [1]. They exist in tow crystallographic phases namely; hexagonal wurtzite or cubic structure [2], possessing an electronic bandgap energy of 3.37 eV and a considerable excitation binding energy



This work is licensed under the Creative Commons Attribution 4.0 International License.

To view a copy of this license, visit <http://creativecommons.org/licenses/by/4.0/>.

amounted to 60 meV at room temperature. ZnO nanoparticles are chemically stable and has excellent electrical and thermal stabilities including high UV absorption properties [3]. Zinc oxide nanoparticles have applications in electronic and instrumental and ceramic industry. It is used in wireless, radio, image recording, piezo electrics, gas sensors, fluorescence lamp, rheostats, electrodes, photonics and acoustics [4].

Zinc oxide nanoparticles (ZnONPs) have biomedical applications due to their unique properties, biocompatibility, and low toxicity [5]. In addition to anticancer, antibacterial treatments [6], antioxidant, antidiabetic and tissue regeneration activities, drug delivery, biosensing, and bioimaging [7,8]. The anticancer and antibacterial effects of ZnONPs are attributed to their ability to produce reactive oxygen species and prompt cell apoptosis [8].

Additionally, ZnONPs showed promise in antidiabetic treatments due to zinc's role in maintaining insulin integrity [9]. In addition to the field of restorative dentistry, endodontics, regenerative endodontics, periodontics, prosthodontics, orthodontics, oral medicine [10,11]. The nanoparticles' excellent luminescent properties make them suitable candidates for bioimaging applications. Furthermore, ZnONPs have been reported to be widely used in industries such as paint products, cosmetics, and textiles [12].

They are commonly used in sunscreens, as they absorb and scatter UV radiation which allow their use in various products. also used in agriculture, which can benefit plant growth but also potentially harm sensitive plant varieties [5], industries and food as well as the environment remediation, biosensors and water purification due to their photocatalytic activity.

ZnONPs have both beneficial and harmful effects, depending on factors like concentration, route of administration, and duration of exposure [13].

The toxic effects of ZnONPs are mediated through the activation of oxidative stress signaling pathways, p53 signaling, and inflammatory pathways [14, and they demonstrate remarkable UV filtering capabilities, photochemical antifungal properties, and high catalytic and antibacterial activities [4].

Various crude medical plants which have excellent chemical component [15,16], extracts

are used for Phytosynthesis NPs, these could be any parts of plants: leaves, roots, stems, flowers, barks or even fruit [17,18]. Bio reduction employing plant resources can either occur intracellularly as plant accumulated metal ion is reduced or extracellularly utilizing crude extract/biomass. Many of them behave as biological reducing in addition to capping agents making them biocompatible and suitable for biomedical applications such as drug delivery and imaging... etc. Plants are reported to be nonpathogenic that is promise most candidates compared to microbes for biogenic synthesis that can easily produce a diversity of nanoparticles [19].

Tannic acid as a type of plant-derived polyphenol enjoys a featured characteristic, including and not limited to, stimulus responsiveness, self-healing, excellent biocompatibility, and biodegradability characteristics [20]. literature has reported that the desired tannic acid structure can easily nominate it to be used as a building block for supramolecular assembled nanostructures in biomedicine [21]. Most importantly, the existence of abundant digalloyl groups accords tannic acid an excellent binding ability for multivalent metal ions [22], leading to fast self-crosslinking of tannic acid in water, producing stable metal ion crosslinked tannic acid nanostructures without extra heating or adding organic solvents, chemicals, or using other certain instrumental tools [23]. Current research is trying to phyto-synthesize zinc oxide NPs using tannic agent as reducing and capping factor, in addition to studying their toxicity to normal and cancer cells.

MATERIALS AND METHODS

Phytosynthesis of Zinc oxide NPs.

Phytosynthesis of ZnONPs was carried out using the method reported by Elumalai *et al.*[24]. In fact, the preparation method was slightly adjusted. Aqueous solution of zinc nitrate (25 mL of 0.013 M), this aqueous solution was heated at a range of temperature from 60 to 80 °C on a magnetic stirrer. As the temperature of solution reached 80°C, the Tannic acid (40 mL of 0.196 mM) was put in ultrasonic device for 5 min [25] and added for nearly 30 min., and the stirring was continued for 12 h when a color change was observed. The mixture had been left for a night in oven at 60 °C till it formed as a creamy paste. This creamy paste was subjected to washing process several times using distilled water and

Ethanol at a ratio of 3:1. Next, the collected paste was put in a ceramic crucible cup in order to be heated in furnace at 200 °C for 2 h. and grounded to fine powder using agate mortar. The resultant white powder was put in an airtight container in order to be experimentally characterized. For characterization, the absorption coefficient (α) and the optical band gap energy (E_g)/ UV-visible, size and distribution of NPs/ AFM, the crystal phases and crystal size / X-ray diffraction, various functional groups/ FTIR, SEM and size, grain size, size distribution and morphology/ TEM and SEM) analysis were determined.

Biological applications

Cytogenetic analysis

The culturing process was carried out to obtain chromosomes analysis according to the method mentioned in Verma and Babu 1989 [26]. Healthy blood people's cultured on (RPMI - 1640) medium. Seven different concentrations of the samples (0.0, 10, 15, 25, 50, 100, 200) $\mu\text{g}/\text{mL}$ were used for analysis. The exposure time and degree temperature were: 37 °C for 70 hours. Mitotic cells MI, Blast index BI and chromosomal aberrations were calculated according to Freshney 1992 [27].

Hemo-compatibility test

This was done according to the Braune et al., 2018 [28] method to determined hemolysis of blood using different concentrations (0.0, 1, 5, 10, 15, 20) $\mu\text{g}/\text{mL}$ ZnONPs.

Cytotoxicity assay against cancer cell line

The HSSC cell line in pass 27 and HOSC cell line in pass 22 were used in anticancer

assay. RPMI-1640 culture medium with all requirements supplemented was used to culture the cell lines. The MTT assay is utilized to inspect cellular metabolic activity as an indicator of cell viability, proliferation and cytotoxicity. Various concentrations of samples/ (0.0, 1, 5, 10, 15, 30, 60, 125, 250, 500, 1000) $\mu\text{g}/\text{mL}$ were applied for inoculation monolayers cell lines as well described in Freshney 1992. The incubation temperature at (37°C), for different exposure periods (24, 48, 72) hours. There were triple replicates, the inhibition rate was calculated according to Freshney 1992 [27].

Statistical analysis

For statistical analysis, analysis of variance (ANOVA) with the least significant differences (LSDs) were used for the analysis statical of the result and P-values at levels ($P \leq 0.01$) were considered to be statically significant. These calculations were carried out according to program SPSS version 10.

RESULTS AND DISCUSSION

Phytosynthesis

In the current study, ZnONPs were prepared utilizing Tannic acid. During Phytosynthesis of ZnONPs, the color of the mixed solution of zinc nitrate and Tannic acid changed from colorless to red color. This color change pointed out that metallic zinc (Zn^{2+}) ions have reduced to zinc oxide ZnONPs, (Fig. 1).

UV-visible spectroscopy

The maximum absorption band for ZnONPs at 268 nm (λ_{max}), which is related to the Surface



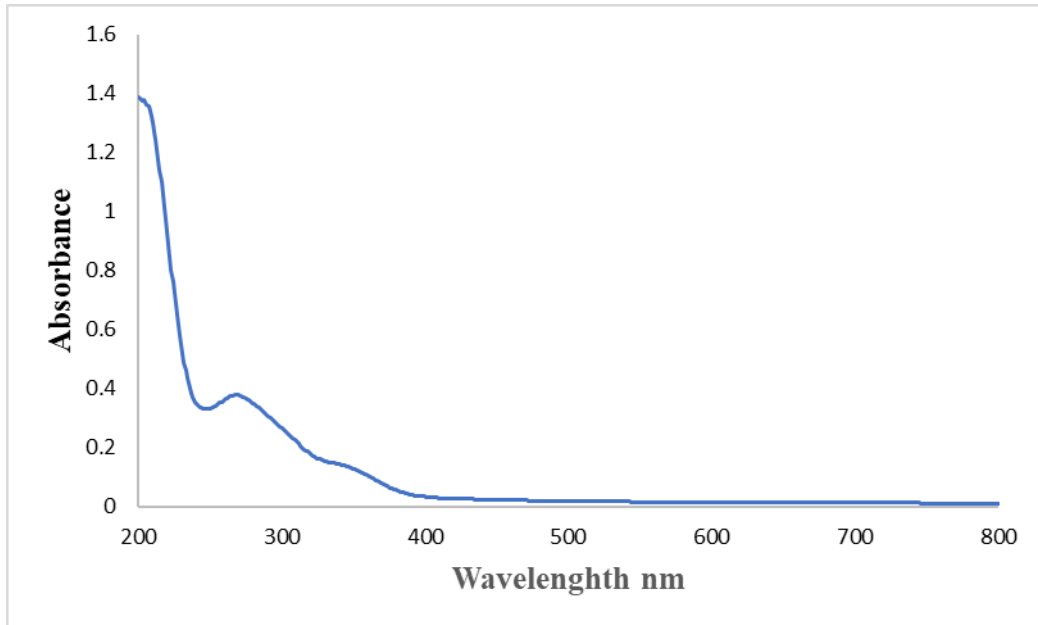
Fig. 1. Color shift during biosynthesis of ZnONPs by tannic acid; (A) Zinc nitrate solution, (B) After annealing solution.

Plasmon Resonance and confirm the formation of ZnONPs in the solution. The band gap energy was computed using $E_g = hc/\lambda$ eVot found that there were four energy band gaps: (0.85, 1.25, 2.45 and 3) eV (Fig. 2). These results are similar and within the range of findings reported by [29-31]

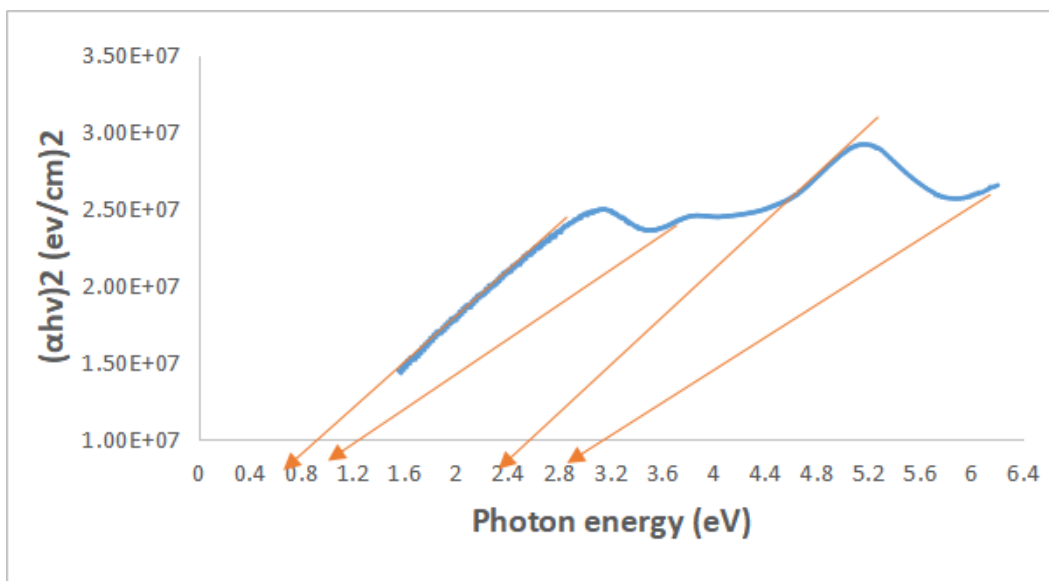
for Phytosynthesized ZnONPs

Fourier transform infrared spectroscopic analysis (FTIR)

The functional groups present on the surface of TA and ZnONPs were investigated by FTIR analysis



(A)



(B)

Fig. 2. (A) absorptions spectrum and (B) $(\alpha h\nu)^2$ versus photon energy of ZnONPs synthesis by tannic acid.

at wavelengths between 4000 cm^{-1} and 400 cm^{-1} (Fig. 3). The functional groups and their stretching which present on the surface of TA were eleven peaks: (430.12, 646, 1028/ strong C-O, 1187 / strong C-O, 1199 /strong C-O, 1400.32, 1448 C-H, 1645.28/strong C=C, 1708 /strong conjugated aldehyde C=O and 3280/ strong alkyne C-H) cm^{-1} . In synthesized ZnONPs, the wide and strong intense band at 420 cm^{-1} which indicates the existence of

ZnO, other functional groups on synthetic ZnONPs with their stretching were: 862.18 strong binding C=H, 1103.28/ strong stretching C-O, 1400.32 medium bending O-H carboxylic acid, 1498.69, 1645.28 strong stretching alkene C=C, 2943.37 medium stretching C-H, 3390.86- O-H All above results were comfortable with Above bands which is stretching to: strong stretching C-O and alkene C=C in addition to medium bending carboxylic acid

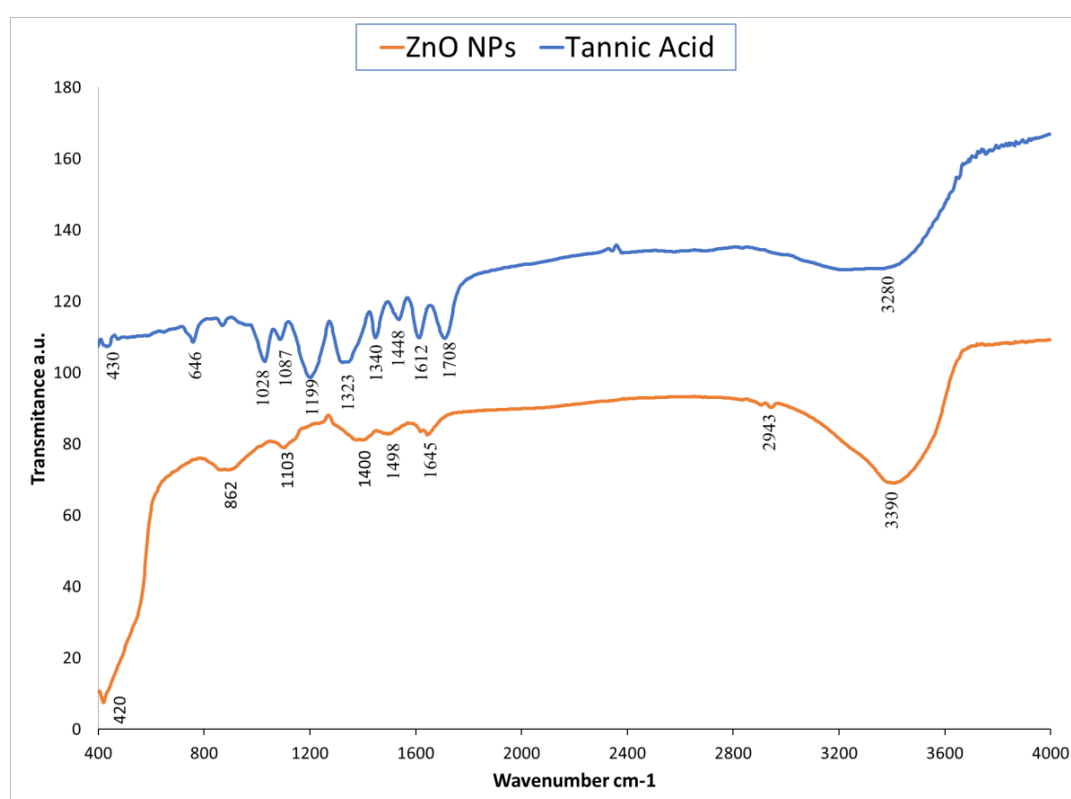


Fig. 3. FTIR analysis of ZnONPs synthesis by tannic acid.

Table 1. XRD characterization of ZnONPs biosynthesis by tannic acid.

plane (h k l)	Pos. [$^{\circ}$ 2 θ .]	FWHM [$^{\circ}$ 2 θ .]	D (NM)	STRAIN XE-4	DIS X1014	Rel. Int. [%]
100	31.895	0.344	23.867	58.072	17.55504	61.1
002	34.5502	0.246	33.648	41.191	8.832363	63.6
101	36.3913	0.344	24.160	57.369	17.13254	100

(hkl) planes: crystallographic plane, (FWHM): Full width at half maximum, (D): dimension of crystallite size, (x10-4): strain value, (x 1014): dislocation density.

and C-H were shifted towards higher or lower than that for in the standard pure of: Tannic acid. These bands are good evidence for the success of the reaction between tannic acid and ZnONPs.

X-ray diffraction

To investigate the crystallographic nature,

structural characteristics and phase purity of the synthesized ZnONPs, XRD analysis was performed, as shown in (Fig. 4). Major diffraction peaks occurring at the 2θ values of (31.847, 34.550, 36.354, 47.694, 56.745, 63.087, 66.558, 68.161, 69.284, 72.870, 77.205, 81.720 and 89.942) were assigned to (100, 002, 101, 102, 110, 103, 200, 112, 201, 202, 104, 203

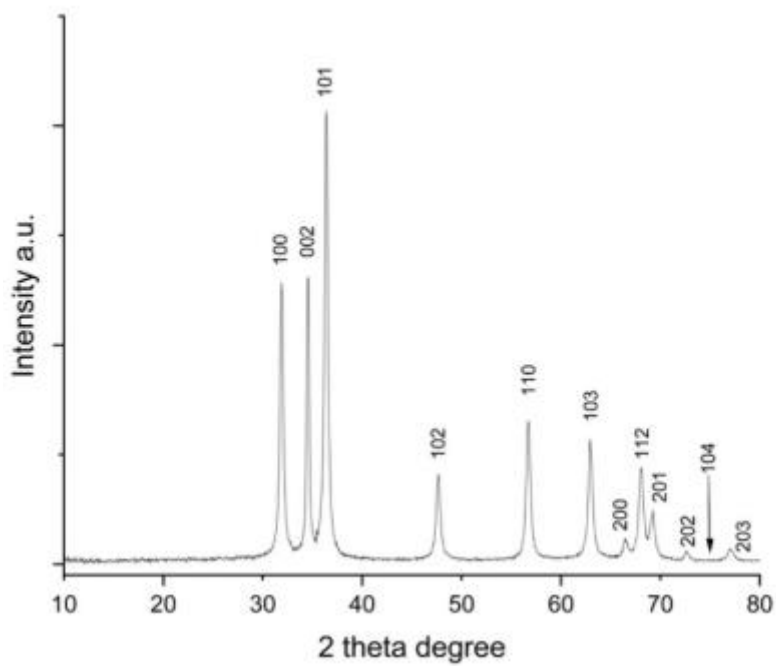


Fig. 4. X-ray pattern of ZnONPs synthesized by tannic acid.

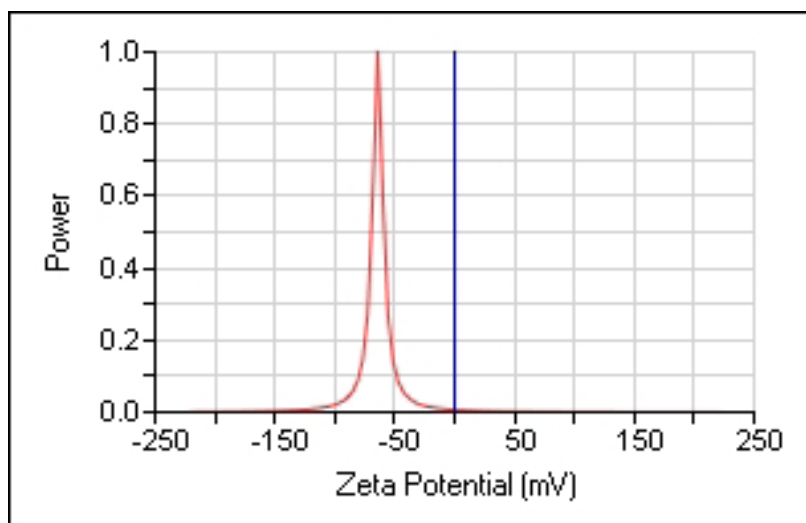


Fig. 5. Zeta potential of ZnONPs synthesis by tannic acid.

201, 004, 202,104 and 203) miller indices plane. A sharp peak at $2\theta = 36.39$ with the diffraction of the (101) plane corresponds to ZnONPs, which indicates that they are hexagonal structure with the space group of C2/c (15). These values agreed well with the standard JCPDS No. 96-210-7060 and with COD database code: 2107059 [32]. Crystal's size, strain value and dislocation density of three optimum peak are shown in (Table 1), average crystals size was: 27.2 nm.

Zeta potential

The colloidal metal nanoparticles' stability is gauged by their zeta potential which is shown by the surface charge of nanoparticles. Greater zeta potential values that inhibit aggregate formation between nanoparticles give nanoparticles their increased stability. Zeta potential was measured at -64.02 mV. (Fig. 5) showed that the produced T.A. Zn nanoparticles were stable, as indicated by the larger negative zeta potential value [33].

Atomic Force Microscopy

The produced ZnONPs' existence and size

distribution were assessed by AFM analysis. Fig. 6 shows the generation of both two-dimensional (2D) and three-dimensional (3D) pictures, the average size was 38.18 nm, root mean square (Sq) of first procedure were: 18.28 nm, maximum height 162.4 nm, Arithmetic mean height 13.84 nm.

SEM

SEM image of ZnONPs which is shown in Fig. 7 found rod shaped particles. Their diameter ranged from 52.67 to 83.74 nm, with some spherical NPs (less than 100 nm), it forms a rough cover. Compared to this study, the morphology of the biosynthesized ZnONPs was presented by Singh et. al. [34] with similar shapes and sizes ranging between 80 and 130nm.

Energy Dispersive X-ray analysis

To obtain additional insight into the topographies and indicated the elemental composition of ZnONPs, the EDX analysis of the sample was performed from the same area as shown in Fig. The EDX analysis confirms the presence of ZnONPs

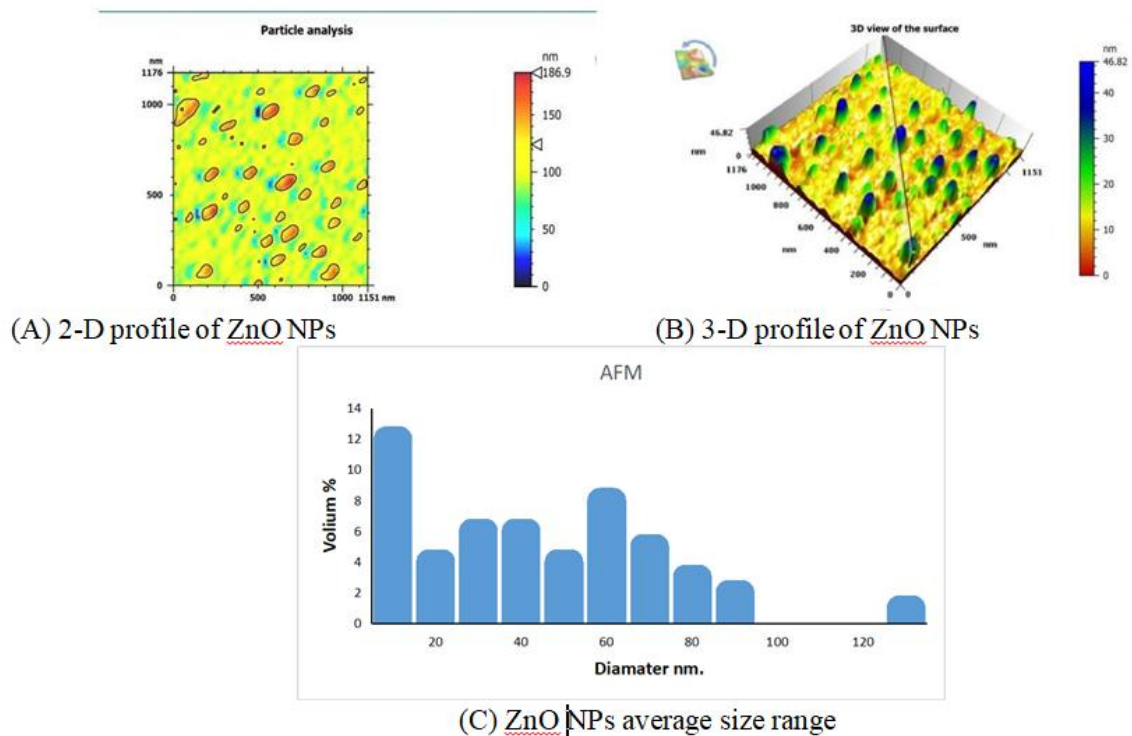


Fig. 6. AFM topographic images. (A) AFM picture of ZnONPs in 2 dimensions; (B) AFM picture of ZnONPs in 3 dimensions; (C) A column AFM diagram showing volume distribution of NPs synthesis by tannic acid.

grown by the phytosynthesized method. The elemental analysis of the ZnONPs yielded 50.52% of zinc and 49.48% of oxygen which proves that the produced ZnONP is in its highest purified form [35,36]. The main components of the ZnONPs are Zn and O content, and also, they are uniformly dispersed on the surface of ZnONPs.

Biological applications

Cytogenetic analysis

Both the Mitotic index (MI) and blastogenic

index (BI) are biological indicators approved and trusted in many studies due to their affected by endogenous and exogenous factors. Cell divisions can be considers the most important indicators of life and activity in living organisms, any physical, chemical or even biological factors that affects this physiological process can lead to the death of the organism, Therefore, these indicators can be used to determine the toxicity of substances based on the degree of their effect on these important vital indicators. The results found significant decreasing

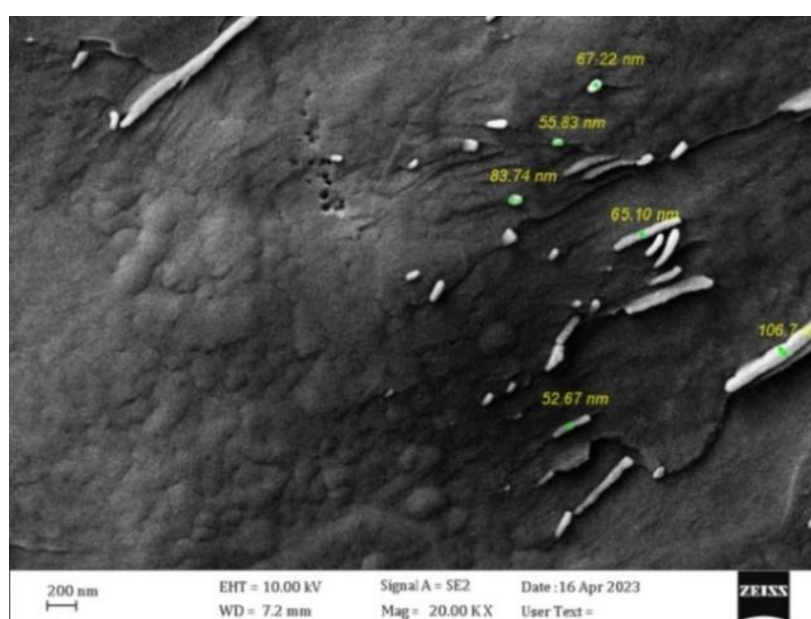


Fig. 7. SEM image of ZnONPs synthesis by tannic acid.

Table 2. Chromosomal analyses in peripheral blood lymphocytes (PBLs) treated with phyto-synthetic ZnONPs.

Con. (µg/mL)	MI	BI	TCA
0	1.45*	66.84*	0.11*
5	1.23 ^a	62.07	0.16 ^a
10	1.11 ^{ab}	60.16	0.18 ^{ab}
15	0.86 ^b	56.96	0.21 ^b
25	0.64	51.35	0.15 ^a
50	0.40	43.49	0 ^c
100	0.22	32.82*	0 ^c
200	0.11	20.78*	0 ^c

The same small letters are nonsignificant at the 0.01 level.

in MI and BI using all concentrations of NPs (Table 2). There were chromosomal aberrations in lymphocyte at all concentrations, significantly at the 0.01 level. MI and BI with concentrations' raising, the significance was apparent in high concentrations more than in low concentrations. As a result of NPs interacting with cell structures, large concentrations of metal oxides cause cell cycle changes, resulting in phase delays which explains the decrease in both MI and BI [37].

Hemo-compatibility test

The results of Table 3 showed cell ZnONPs interactions cause significant erythrocyte aggregation with damaging consequences, despite the NPs having significant hemolytic activity.

NPs can easily access these cells and influence both their structure and function that can result in potentially toxic effects. Therefore, researchers should make every effort to conduct thorough hemocompatibility studies on newly engineered NPs that evaluate the interactions between the NPs and all three cellular constituents of blood

[38]. However, the methods whereby NPs interact with erythrocytes to cause hemolysis has not been fully elucidated. Deferent mechanisms have been suggested, including interactions with the erythrocyte membrane, cellular uptake, internalization and oxidative stress. The most prominent mechanism is the direct interaction of NPs with the erythrocyte membrane which can lead to injury, detrimental morphological changes and cytoskeletal distortion [39].

Cytotoxicity assay against cancer cell line Human oral squamous carcinoma cell line.

The results showed a significant difference at the level of 0.01 between the control and all treatments when incubated for a period of 24, 48, and 72 hours, except for the lowest concentration of 1 µg/mL, which did not differ significantly with the control for two incubation periods of 24.48 hours.

All concentrations higher than 10 µg/mL were significant when compared among themselves for the incubation period of 24 hours. The same

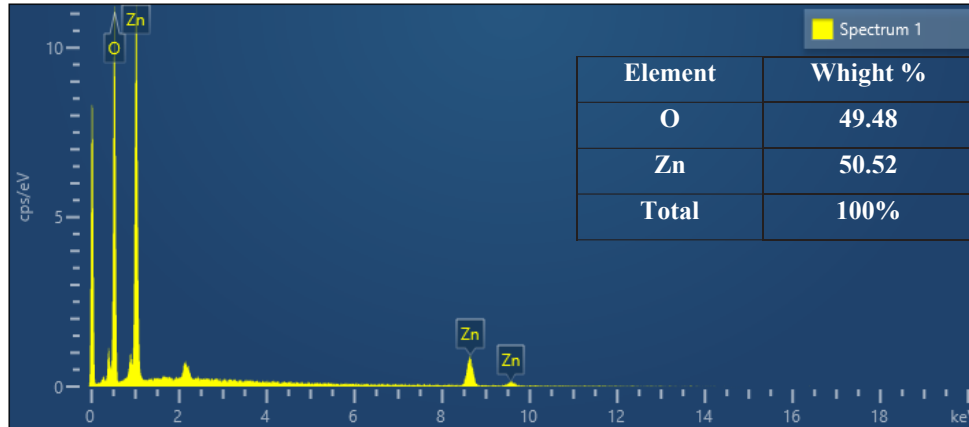


Fig. 8. EDX spectrum of the ZnONPs.

Table 3. Hemo-compatibility test.

Con. µg/mL	ZnONPs	
	Ab	H%
+ve	0.658	100
-ve	0.00	0.0
1	0.00	0.0
5	0.009	1.36
10	0.012	1.82
15	0.017	2.58
20	0.021	3.19

pattern appeared when incubated for a period of 48 hours, except for the concentration of 10 µg/mL, which was significant with the other

concentrations. When the incubation period was increased to 72 hours, all concentrations appeared significant when compared with each other.

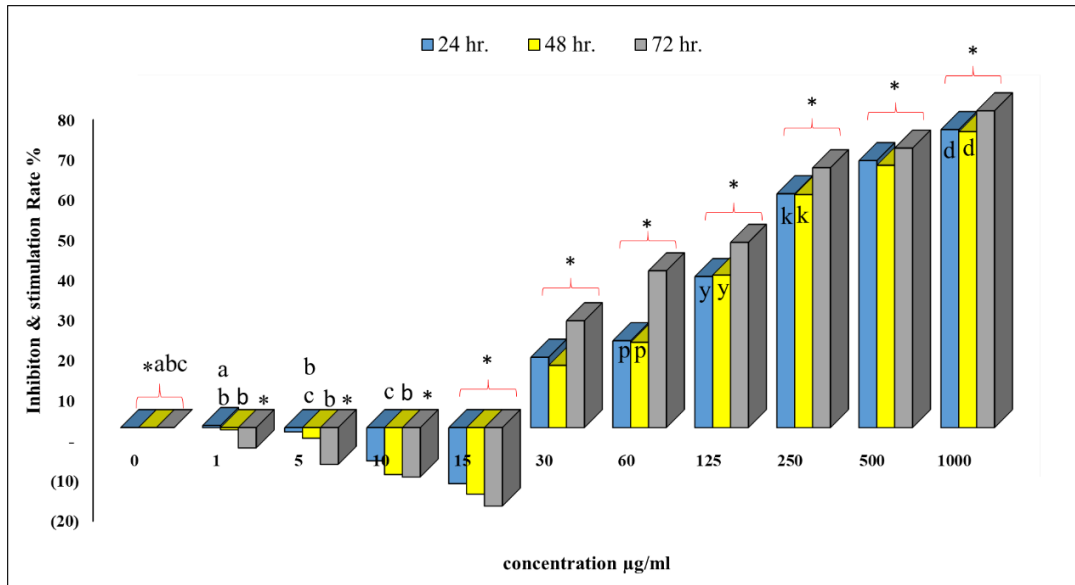


Fig. 9. Cytotoxicity assay of Phyto-synthetic ZnONPs against human oral squamous carcinoma cell line, *: The mean difference is significant at the 0.01 level compared with all other treatments. The similar small letters are non-significant at the 0.01 level compared with the same concentration and exposure time.

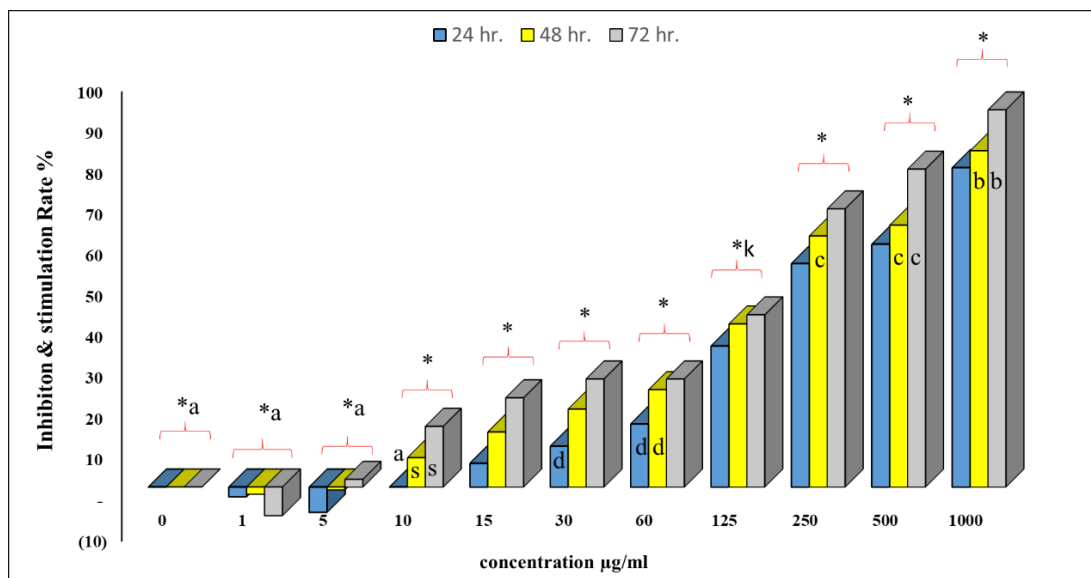


Fig. 10. Cytotoxicity assay of Phyto-synthetic ZnONPs against human skin squamous carcinoma cell line, *: The mean difference is significant at the 0.01 level compared with all other treatments. The similar small letters are non-significant at the 0.01 level compared with the same concentration and exposure time.

The results showed that there were significant differences between most of the concentrations incubated for 24 hours and between the same concentrations that were incubated for 48 and 72 hours, and that the 72-hour incubation period was lethal and significant with the rest of the incubation periods.

The nanoparticles had a hormetic effect, as concentrations of 1-15 stimulated the growth of cancer cells significantly at a level of 0.01 compared to the control, while concentrations higher than 15 $\mu\text{g}/\text{mL}$ were significantly inhibitory to growth when incubated for 24 hours.

The IC_{50} was 200, 200, and 150 $\mu\text{g}/\text{mL}$ for incubation periods of 24, 48, and 72 hours, respectively (Fig. 9).

The hermetic effect of a substance is described as a biphasic dose-response to an environmental or chemical agent with a low dose stimulation or favorable effect and a high dose inhibitory or toxic effect on the cells or organisms [40].

Human skin squamous carcinoma cell line

The results showed that all concentrations higher than 5 $\mu\text{g}/\text{mL}$ were significant when compared to the control for the three incubation periods (Fig. 8). Comparing these concentrations with each other, all doses is significant at the incubation period of 72 hours while the significance depends mainly on the concentration and time for both incubation periods of 24-48 hours. The IC_{50} was 225, 182, and 167 $\mu\text{g}/\text{mL}$ for incubation periods of 24, 48, and 72 hours, respectively.

The physical and chemical features of nanomaterials have a significant impact on the uptake and drug distribution in the tumor cell. The size of the NPs allows the easier tumor cell membrane penetration. Nanomaterials can bind to the surface of biological membranes through forces of electrostatic attraction and adsorption. They can harm the cells by releasing reactive oxygen species, which can cause protein denaturation and DNA damage which leads to the cell death [41,42].

CONCLUSION

In the present study, hexagonal structure nanoparticles of ZnONPs were synthesized using Tannic acid. There is good evidence for the success of the reaction between tannic acid and ZnONPs having four energy band gaps indicating to presence of two quantitative wells.

The zinc oxide nanoparticles that were prepared were inhibit the growth of HSSC cell line and HOSC at various periods of incubation of 24, 48, and 72 hours. Ther were evident that the higher concentration of ZnONPs found to inhibit mitotic index, blastogenic index and caused chromosomal aberrations in blood lymphocytes. Further studies can be conducted on how to reduce the toxicity of this nanomaterial by coating it with biocompatible molecules.

ACKNOWLEDGMENTS

The authors would like to thank Al-Mustansiriyah University (www.uomustansiriyah.edu.iq) Baghdad Iraq for its support in the present work.

CONFLICT OF INTEREST

The authors declare that there is no conflict of interests regarding the publication of this manuscript.

REFERENCES

1. Dagdag O, Haldhar R, Quadri TW, Daoudi W, Berdimurodov E, Kim H. Nanomaterials and Their Properties. ACS Symposium Series: American Chemical Society; 2024. p. 17-40.
2. Satdev, Zinzala VJ, Saini LK, Chauhan AR. Synthesis and characterization of zinc oxide nanoparticles (ZnO-NPs) via precipitation method. Journal of Pharmacognosy and Phytochemistry. 2020;9(2):304-307.
3. Aswathi VP, Meera S, Maria CGA, Nidhin M. Green synthesis of nanoparticles from biodegradable waste extracts and their applications: a critical review. Nanotechnology for Environmental Engineering. 2022;8(2):377-397.
4. Krishnan K. Pharmaceutical and Biomedical Applications of Zinc Oxide Nanoparticles. Zinc: CRC Press; 2024. p. 240-254.
5. Czyżowska A, Barbasz A. A review: zinc oxide nanoparticles – friends or enemies? Int J Environ Health Res. 2020;32(4):885-901.
6. Motelica L, Vasile B-S, Ficai A, Surdu A-V, Ficai D, Oprea O-C, et al. Antibacterial Activity of Zinc Oxide Nanoparticles Loaded with Essential Oils. Pharmaceutics. 2023;15(10):2470.
7. Singh TA, Sharma A, Tejwan N, Ghosh N, Das J, Sil PC. A state of the art review on the synthesis, antibacterial, antioxidant, antidiabetic and tissue regeneration activities of zinc oxide nanoparticles. Advances in Colloid and Interface Science. 2021;295:102495.
8. Abd-Elmaqsoud I, Elsaadawi H, Ahmed A, AbdelKhalek A, Arisha A. The Vast Biomedical Applications of Zinc Oxide Nanoparticles. Zagazig Vet J. 2022;50(3):201-218.
9. Jiang J, Pi J, Cai J. The Advancing of Zinc Oxide Nanoparticles for Biomedical Applications. Bioinorg Chem Appl. 2018;2018:1062562-1062562.
10. Pushpalatha C, Suresh J, Gayathri VS, Sowmya SV, Augustine D, Alamoudi A, et al. Zinc Oxide Nanoparticles: A Review on Its Applications in Dentistry. Frontiers in bioengineering and biotechnology. 2022;10:917990-917990.
11. El-Gebaly AS, Sofy AR, Hmed AA, Youssef AM. Green synthesis, characterization and medicinal uses of silver nanoparticles (Ag-NPs), copper nanoparticles (Cu-NPs) and

- zinc oxide nanoparticles (ZnO-NPs) and their mechanism of action: A review. *Biocatalysis and Agricultural Biotechnology*. 2024;55:103006.
12. Kumawat A, Misra KP, Chattopadhyay S. Band Gap Engineering and Relationship with Luminescence in Rare-Earth Elements Doped ZnO: An Overview. *Materials Technology*. 2022;37(11):1595-1610.
 13. Zinc Oxide Nanoparticles Synthesis Methods and its Effect on Morphology: A Review. *Biointerface Research in Applied Chemistry*. 2021;12(3):4261-4292.
 14. Keerthana S, Kumar A. Potential risks and benefits of zinc oxide nanoparticles: a systematic review. *Crit Rev Toxicol*. 2020;50(1):47-71.
 15. Jalill RDA. Chemical analysis and anticancer effects of Juniperus polycarpus and oak gall plants extracts. *Research Journal of Pharmacy and Technology*. 2018;11(6):2372.
 16. Jalill RDA, Jaber TF, Jalal ZJ, Al-Araji AR. Cytotoxicity and chemical analysis of oil seeds of Citrullus colocynthis. *Medicinal Plants - International Journal of Phytomedicines and Related Industries*. 2018;10(3):216.
 17. Mohamed M, Gouda G, Nagiub A. Biosynthesis and antibacterial evaluation of zinc oxide nanoparticles from Onion extract (Allium cepa). *Bulletin of Pharmaceutical Sciences Assiut*. 2023;0(0):0-0.
 18. *Green Metal Nanoparticles*: Wiley; 2018.
 19. Kulkarni D, Sherkar R, Shirsathe C, Sonwane R, Varpe N, Shelke S, et al. Biofabrication of nanoparticles: sources, synthesis, and biomedical applications. *Frontiers in bioengineering and biotechnology*. 2023;11:1159193-1159193.
 20. Chowdhury P, Nagesh PKB, Hatami E, Wagh S, Dan N, Tripathi MK, et al. Tannic acid-inspired paclitaxel nanoparticles for enhanced anticancer effects in breast cancer cells. *Journal of colloid and interface science*. 2019;535:133-148.
 21. Liu L, Ge C, Zhang Y, Ma W, Su X, Chen L, et al. Tannic acid-modified silver nanoparticles for enhancing anti-biofilm activities and modulating biofilm formation. *Biomaterials Science*. 2020;8(17):4852-4860.
 22. Hasi RY, Ali H, Islam M, Habib R, Satter MA, Yeasmin T. Antioxidant and antineoplastic activities of roots of Hibiscus sabdariffa Linn. Against Ehrlich ascites carcinoma cells. *Clinical Phytoscience*. 2019;5(1).
 23. Che Lah NA, Kamaruzaman A, Trigueros S. pH-Dependent Formation of Oriented Zinc Oxide Nanostructures in the Presence of Tannic Acid. *Nanomaterials (Basel, Switzerland)*. 2020;11(1):34.
 24. Elumalai K, Velmurugan S, Ravi S, Kathiravan V, Ashokkumar S. Retraction notice to "Green synthesis of Zinc oxide nanoparticles using Moringa oleifera leaf extract and evaluation of its antimicrobial activity" [Spectrochim. Acta A Mol. Biomol. Spectrosc. 143 (2015) 158-164]. *Spectrochimica Acta Part A: Molecular and Biomolecular Spectroscopy*. 2019;206:651.
 25. Abdul Jalill RD. Green synthesis of titanium dioxide nanoparticles with volatile oil of Eugenia caryophyllata for enhanced antimicrobial activities. *IET nanobiotechnology*. 2018;12(5):678-687.
 26. Human chromosomes. *Manual of basic techniques*. Japanese journal of human genetics. 1990;35(1):117-117.
 27. Dawson M. *Animal cell culture ? a practical approach* edited by R. I. Freshney, IRL Press at Oxford University Press, 1992. UKE19.50 (xix + 329 pages) ISBN 0 19 963213 8. *Trends Biotechnol*. 1993;11(10):437.
 28. Braune S, Lendlein A, Jung F. Developing standards and test protocols for testing the hemocompatibility of biomaterials. *Hemocompatibility of Biomaterials for Clinical Applications*: Elsevier; 2018. p. 51-76.
 29. Selim YA, Azb MA, Ragab I, H M Abd El-Azim M. Green Synthesis of Zinc Oxide Nanoparticles Using Aqueous Extract of Deverra tortuosa and their Cytotoxic Activities. *Sci Rep*. 2020;10(1):3445-3445.
 30. Lyimo GV, Ajayi RF, Maboza E, Adam RZ. A green synthesis of zinc oxide nanoparticles using Musa Paradisiaca and Rooibos extracts. *MethodsX*. 2022;9:101892-101892.
 31. Elbrolesy A, Abdou Y, Elhussiny FA, Morsy R. Novel Green Synthesis of UV-Sunscreen ZnO Nanoparticles Using Solanum Lycopersicum Fruit Extract and Evaluation of Their Antibacterial and Anticancer Activity. *Journal of Inorganic and Organometallic Polymers and Materials*. 2023;33(12):3750-3759.
 32. Albertsson J, Abrahams SC, Kwick Å. Atomic displacement, anharmonic thermal vibration, expansivity and pyroelectric coefficient thermal dependences in ZnO. *Acta Crystallographica Section B Structural Science*. 1989;45(1):34-40.
 33. Ahmed HM, Sobhy NA, Ibrahim WA, Fawzy ME. Green Biosynthesis of zinc Oxide Nanoparticles Utilizing Pomegranate Peel Extract for Grey Water Treatment. *Solid State Phenomena*. 2023;342:27-36.
 34. Singh TA, Das J, Sil PC. Zinc oxide nanoparticles: A comprehensive review on its synthesis, anticancer and drug delivery applications as well as health risks. *Advances in Colloid and Interface Science*. 2020;286:102317.
 35. Yedurkar S, Maurya C, Mahanwar P. Biosynthesis of Zinc Oxide Nanoparticles Using Ixora Coccinea Leaf Extract—A Green Approach. *Open Journal of Synthesis Theory and Applications*. 2016;05(01):1-14.
 36. Shnawa BH, Hamad SM, Barzinjy AA, Kareem PA, Ahmed MH. Scolicidal activity of biosynthesized zinc oxide nanoparticles by Mentha longifolia L. leaves against Echinococcus granulosus protoscolices. *Emergent Materials*. 2021;5(3):683-693.
 37. Size Control of Ag Nanoparticles Synthesized by PLA Method in Different Liquid Environments and their Potent against Virulent Candida Albicans. *Journal of Pharmaceutical Negative Results*. 2022;13(4).
 38. de la Harpe KM, Kondiah PPD, Choonara YE, Marimuthu T, du Toit LC, Pillay V. The Hemocompatibility of Nanoparticles: A Review of Cell-Nanoparticle Interactions and Hemostasis. *Cells*. 2019;8(10):1209.
 39. Haleem AM, Hameed AH, Al-Majeed RA, Hussein NN, Hikmat RA, Queen BK. Anticancer, Antioxidant, Antimicrobial and Cytogenetic Effects of Ethanol Leaves Extract of Carthamus tinctorius. *IOP Conference Series: Earth and Environmental Science*. 2023;1262(5):052035.
 40. Günes-Bayir A, Kocyigit A, Guler EM, Dadak A. In Vitro Hormetic Effect Investigation of Thymol on Human Fibroblast and Gastric Adenocarcinoma Cells. *Molecules (Basel, Switzerland)*. 2020;25(14):3270.
 41. Das CGA, Kumar VG, Dhas TS, Karthick V, Kumar CMV. Nanomaterials in anticancer applications and their mechanism of action - A review. *Nanomed Nanotechnol Biol Med*. 2023;47:102613.
 42. Haleem AM, Taha MM, Ayoub AA. Anti-tumor and anti-oxidant effects of Ganoderma lucidum extracts on oral squamous cell carcinoma and skin squamous cell carcinoma in vitro. *Current Issues in Pharmacy and Medical Sciences*. 2024;37(2):79-84.